

Three-Dimensional Elastic Compatibility: Twinning in Martensites

K. Ø. Rasmussen, T. Lookman, A. Saxena, A. R. Bishop, and R. C. Albers
Theoretical Division, Los Alamos National Laboratory, Los Alamos, New Mexico 87545

We show how the St.Venant compatibility relations for strain in three dimensions lead to twinning for the cubic to tetragonal transition in martensitic materials within a Ginzburg-Landau model in terms of the six components of the symmetric strain tensor. The compatibility constraints generate an anisotropic long-range interaction in the order parameter (deviatoric strain) components. In contrast to two dimensions, the free energy is characterized by a “landscape” of competing metastable states. We find a variety of textures, which result from the elastic frustration due to the effects of compatibility. Our results are also applicable to structural phase transitions in improper ferroelastics such as ferroelectrics and magnetoelastics, where strain acts as a secondary order parameter.

81.30.Kf, 64.70.Kb, 61.72.Dc, 82.65.Dp

Strain plays a crucial role in many structural phase transitions, either as a primary order parameter (OP), e.g., in technologically important martensites [1] and shape memory alloys [2], or as a secondary OP, e.g., in ferroelectric [3] and magnetoelastic [4] materials. Moreover, self-consistent coupling of strain to either charge (e.g., high-temperature superconductors [5]) or spin (e.g., colossal magnetoresistance manganites [6]) degrees of freedom determines key physical properties. However, the physical degrees of freedom in a continuum elastic medium (such as described by Ginzburg-Landau models) are contained in the displacement field, $u(r)$, even though it is the strain fields, ϵ_{ij} , which appear in the free energy. Instead of treating the strains as independent fields, one must assume that they correspond to a physical displacement field, i.e., they are derivatives of a single continuous function. This is achieved by requiring that they satisfy a set of nontrivial (Saint-Venant) compatibility relations concisely expressed by the equation $\nabla \times (\nabla \times \epsilon) = 0$ [7] (in the absence of voids, dislocations, etc.). Indeed, ignoring the geometrical compatibility constraint and minimizing the free energy directly would lead to the erroneous result that non-OP strain components are identically zero, and that the OP responds trivially to perturbations, such as stress or local disorder, which is incorrect.

We show for the first time that a consistent Ginzburg-Landau (GL) understanding of martensitic textures in terms of the OP-strain alone, and involving long-range OP strain-strain forces, is possible in three dimensions (3D). A 3D free energy expressed entirely in the order parameter strain variable(s), rather than the displacement field, provides a unified understanding of martensitic textures. We use 3D compatibility equations, linking the strain tensor components in the bulk and at interfaces, that induce anisotropic order-parameter strain interactions (*masked* in a conventional displacement-field treatment). These two long-range bulk and interface potentials, together with local compositional fluctuations, drive the formation of global elastic textures. In contrast to 2D, the rich microstructure is the result of frustra-

tion and competing metastable states in a complicated energy landscape. Here we will focus only on twinning for illustrative purposes. Other complex textures follow from our formalism and will be reported elsewhere. Our work is an essential step towards understanding results of High Resolution Electron Microscopy (HREM) and neutron scattering studies in alloys such as FePd and NiAl. In Fe_xPd_{1-x} , (011) twins preferentially grow at the expense of (101) twins as the temperature is gradually lowered to the martensitic transition temperature [8]. In Ni_xAl_{1-x} , martensite forms with a long period stacking structure involving (110) planes [9]. Due to the directional aspects of the long-range interactions encoded by the underlying symmetry of the lattice, our analysis predicts such twinning planes and directions.

Model. As a specific example, we examine a cubic to tetragonal transition. In this case the symmetry-adapted strains e_i can be defined in terms of the Lagrangian strain tensor components ϵ_{ij} as the dilatation $e_1 = (1/\sqrt{3})(\epsilon_{11} + \epsilon_{22} + \epsilon_{33})$, the deviatoric (i.e., OP) strains $e_2 = (1/\sqrt{2})(\epsilon_{11} - \epsilon_{22})$, $e_3 = (1/\sqrt{6})(\epsilon_{11} + \epsilon_{22} - 2\epsilon_{33})$ and the three shear strains $e_4 = 2\epsilon_{23}$, $e_5 = 2\epsilon_{13}$, $e_6 = 2\epsilon_{12}$. The elastic energy in 3D is given by [10]

$$F = F_L(e_2, e_3) + F_{grad}(\nabla e_2, \nabla e_3) + F_{cs}(e_1, e_4, e_5, e_6),$$

where the Landau free energy (Fig. 1), which provides the driving force for the transition, is

$$F_L = A(e_2^2 + e_3^2) + B e_3(e_2^2 - 3e_3^2) + C(e_2^2 + e_3^2)^2,$$

and the Ginzburg (or gradient) contribution, which is responsible for the interfacial energies, to the free energy is

$$\begin{aligned} F_{grad} = g & \left[(e_{2,x}^2 + e_{2,y}^2) + \frac{1}{3}(e_{3,x}^2 + e_{3,y}^2) \right. \\ & \left. + \frac{2}{\sqrt{3}}(e_{2,x}e_{3,x} - e_{2,y}e_{3,y}) + \frac{4}{3}e_{3,z}^2 \right] \\ & + h \left[(e_{3,x}^2 + e_{3,y}^2) + \frac{1}{3}(e_{2,x}^2 + e_{2,y}^2) \right] \end{aligned}$$

$$- \frac{2}{\sqrt{3}}(e_{2,x}e_{3,x} - e_{2,y}e_{3,y}) + \frac{4}{3}e_{2,z}^2 \Big]$$

The harmonic elastic energy contribution due to non-OP compression-shear (CS) strain components is

$$F_{cs} = A_c e_1^2 + A_s (e_4^2 + e_5^2 + e_6^2).$$

It is also possible to add a coupling, $F_{compos}(\eta, \nabla\eta, e_2, e_3)$, of the OP strain to compositional fluctuations η , which are responsible for tweed, but we do not consider such effects in the present paper.

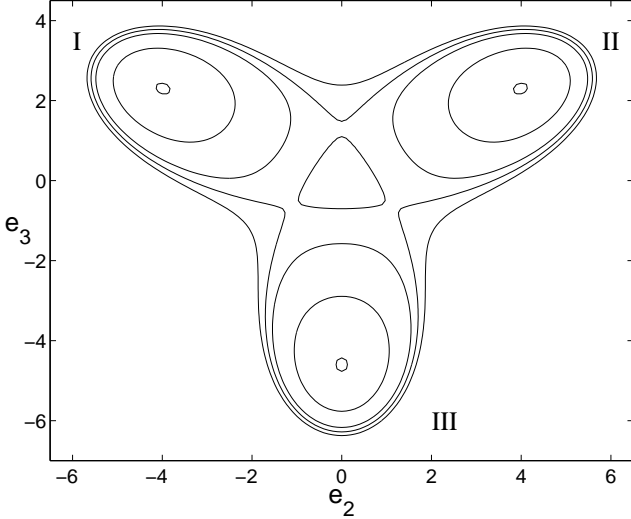


FIG. 1. Countour plot of the Landau free energy in the martensite phase depicting the three degenerate energy minima corresponding to the three tetragonal variants with tetragonal axis along the x , y and z axis, respectively. Parameters are $A = -1.0$, $B = 0.83$ and $C = 0.04$.

The coefficients $A = A_o(T - T_o)$, B and C are related to the second, third and fourth order elastic constants, respectively, and can be obtained from experimental structural data. The martensitic transition temperature is denoted T_o and the gradient coefficients g and h are determined from the phonon dispersion at the appropriate high-symmetry point in the Brillouin zone of the material. A_c and A_s denote the bulk compression and shear moduli, respectively. Here we do not consider the gradient energy contribution from the non-OP components e_1 , e_4 , e_5 , and e_6 , since their contribution is of secondary nature compared to the terms reported above.

3D compatibility and analysis. We express the non-OP strains in terms of the OP strains (e_2 , e_3) using the three compatibility constraints $\epsilon_{12,12} = \epsilon_{11,22} + \epsilon_{22,11}$, $\epsilon_{23,23} = \epsilon_{22,33} + \epsilon_{33,22}$, $\epsilon_{31,31} = \epsilon_{33,11} + \epsilon_{11,33}$. Analogous to the 2D case [12] the constrained minimization of the compression-shear energy leads to an *anisotropic long-range interaction* between the OP strains in the bulk:

$$F_{cs}^{bulk} = \int d^3r e_\alpha(\alpha) U_{\alpha\alpha'}(|r - r'|) e_{\alpha'}(r') \quad (\alpha, \alpha' = 2, 3),$$

where the kernels U_{22} , U_{23} , and U_{33} can be expressed explicitly in Fourier space with each of the three kernels becomes a ratio of algebraic combinations of k_x , k_y and k_z . All these combinations have the same order in the length, k , of the wavevector \vec{k} . Hence, the kernels do not have any scale dependence. That is, the kernels only depend on the angles ϕ and θ , defined in terms of spherical coordinates. The minima of each kernel occur at certain θ and ϕ values. These angles vary from kernel to kernel and the system, in general, experiences frustration. Figure 2 shows contours of the kernel U_{22} and U_{33} as functions of the two angles θ and ϕ . The minima define a direction in 3D in which the compression-shear energy arising from the particular kernel is minimal.

In contrast to 2D, F_{cs} can be viewed as a weighted sum of the three kernels, where the fields e_2 and e_3 act as the weights. There is thus an interplay between F_L and the directional dependence of F_{cs} to accommodate the frustration and choose minima, which in general do not have zero energy. Thus, there exist metastable minima corresponding to different microstructures. In 2D there is no such interplay, as the directional minimum is independent of the amplitude of the field: There is only one minimum corresponding to zero energy and hence there is no frustration. Moreover, these long-range kernels in 3D fulfill the full cubic symmetry properties associated with the transformation. In particular, F_{cs} is invariant with respect to two-fold, three-fold, and four-fold rotation symmetries of the cube. We do not present here the mathematical structure underpinning this, but it is reflected in the frustration seen in 3D that is lacking in 2D.

The bulk contribution comes from a solid with periodic boundaries while the effects of interfaces/surfaces such as habit planes (i.e., austenite-martensite or parent-product boundaries) may be included through a free energy contribution, F_{cs}^{surf} , where $F_{cs} = F_{cs}^{bulk} + F_{cs}^{surf}$ and [12]

$$F_{cs}^{surf} = \int d^3k \Gamma(k_x, k_y, k_z) [e_2(k)^2 + e_3(k)^2].$$

In analogy with the 2D case the function $\Gamma(\vec{k})$ has the form

$$\Gamma(\vec{k}) = \nu \left[\frac{1}{|k_x \pm k_y|} + \frac{1}{|k_y \pm k_z|} + \frac{1}{|k_z \pm k_x|} \right]$$

for the [110] family of habit planes.

We remark that the physics of twinning is quite different in 2D and 3D. In 2D both the gradient and the bulk compatibility terms vary as $\sim 1/r^2$ and thus do not lead to a length scale. However, the surface compatibility term in 2D is essential for introducing a length scale. It varies as $\sim 1/r$ which then competes with the combined bulk compatibility and gradient terms to give rise

to a twinning width. In 3D, the gradient terms behave as $\sim 1/r^2$ and $F_{cs}^{bulk} \sim 1/r^3$. Thus, there is already a length scale present and F_{cs}^{surf} merely renormalizes the length scale arising from the bulk compatibility and gradient terms. We have numerically verified the above scaling relations. On the basis of the above arguments we expect the twin width to scale as the square-root of the length in 3D to hold on the basis of above arguments.

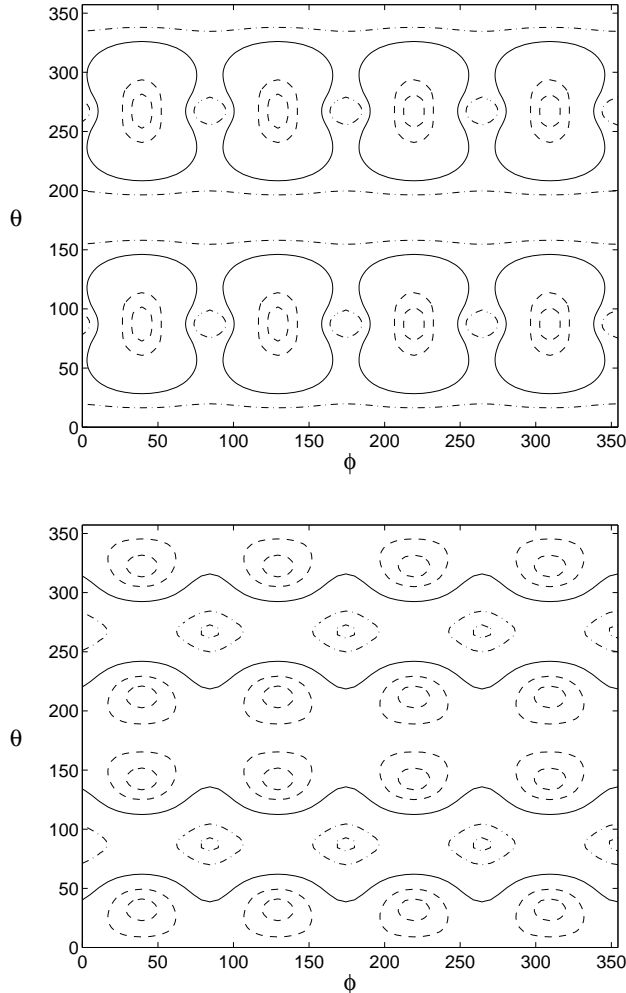


FIG. 2. Three dimensional compatibility kernels U_{22} (upper) and U_{33} (lower) as a function of the colatitude θ and the azimuth ϕ angles. Dashed contours surround minima, and dashed dotted surround maxima, while solid contours show intermediate levels. The parameters are $A_s = 1.2$ and $A_c = 2.4$.

Texture simulations. The various martensitic textures that realize minima of the energy are found from random initial conditions and relaxational dynamics for the OP strains. That is, $\dot{e}_\alpha(r) = -\frac{\delta F(e_\alpha, e_1(e_\alpha), e_4(e_\alpha), e_5(e_\alpha), e_6(e_\alpha))}{\delta e_\alpha(r)}$, where the time t is scaled with a characteristic relaxation rate and $\alpha = 2, 3$. Depending on the details of the initial configurations, various twinning textures reflecting the metastability

emerge as \dot{e}_α vanishes. The simulations are performed for a regular cube, and periodic boundary conditions are applied in all six directions to obtain fully relaxed textures in $e_2(r)$ and $e_3(r)$.

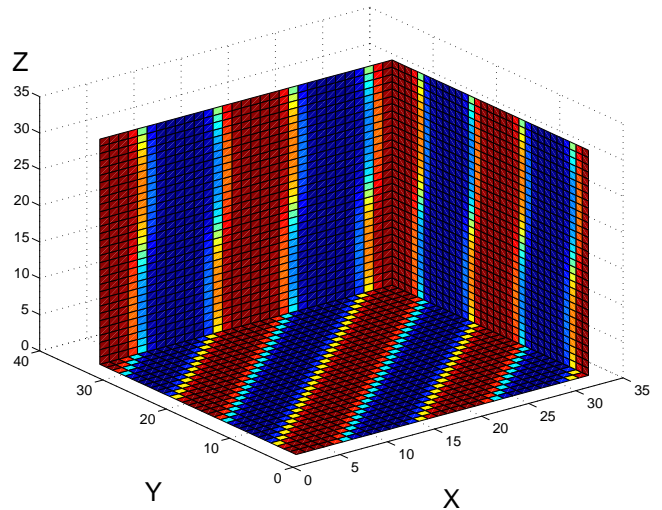


FIG. 3. (Color) Three dimensional twins in the (110) plane obtained from the time-dependent Ginzburg-Landau simulations, with representative parameters as given in Figs. 1 and 2 and, $h = 1$ and $g = 1$. The scale of the twins is determined by the competition between the interfacial energy and the bulk compression-shear energy, whereas the sharpness of the domain walls is determined by the Landau energy.

We illustrate the simulation results obtained with representative (scaled) parameters. The red/blue/green color represent (e_2, e_3) positive/negative/zero OP strain values, respectively (the actual values are approximately determined by the minima of F_L as illustrated in Fig.1).

Figure 3 shows the simplest twinning texture ((110) twins) that is uniform in the z direction. The strain e_2 changes from negative (minimum I in Fig. 1) to positive (minimum II in Fig. 1) (i.e. blue to red). The strain e_3 is not shown, as it is essentially constant with a small modulation at the twin boundaries. This particular martensitic texture is the trivial extension of the 2D results since the OP fields are uniform in the z directions. Notice also that the directional dependence is the same as observed in 2D studies [12].

A richer texture is shown in Fig. 4, where the strain e_3 changes from negative (minimum III in Fig. 1) to positive (minimum I or II in Fig. 1) (i.e. blue to red). The strain e_2 would either be zero (green) when e_3 is negative (minimum III) or positive/negative when e_3 is positive. The figure clearly shows that twins with strain e_2 can be oriented in two possible ways. This reflects the inversion symmetry of the kernels with respect to x, y . We note that a similar alternating twin microstructure has been implied by neutron and x-ray scattering studies in

layered high-temperature superconductors [5].

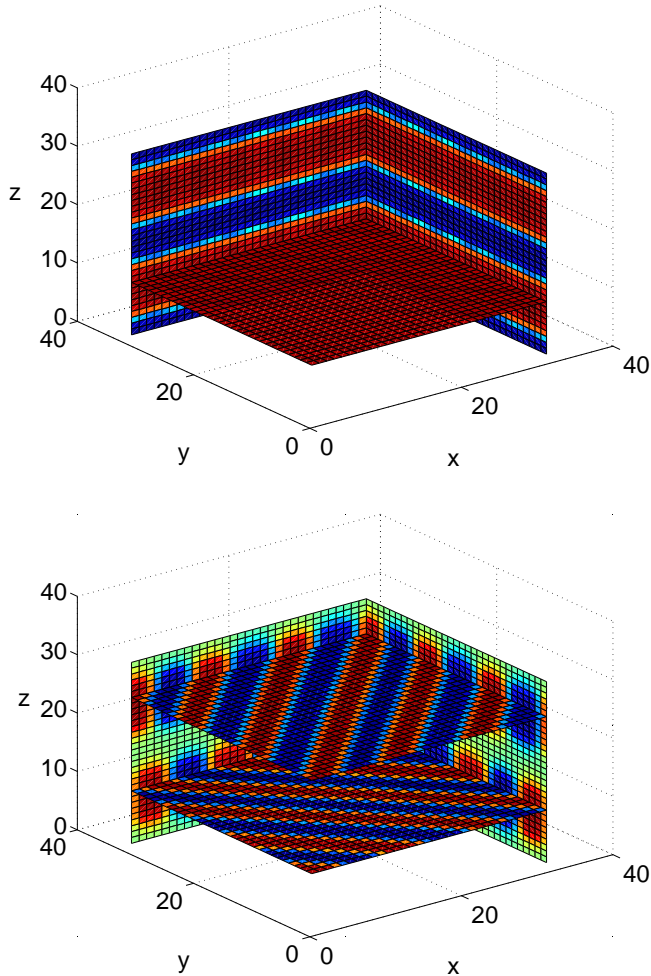


FIG. 4. (Color) Three dimensional twins with two different orientations, (110) and $(\bar{1}\bar{1}0)$, in adjacent planes. Both OP fields are shown, e_3 in the upper panel and e_2 in the lower.

To illustrate the of frustration that is inherent in the compatibility relations, we explain the orientation of the twins in Fig. 4. We construct an effective kernel for the red and blue twins, respectively, using the appropriate values of the strains e_2 and e_3 in the twins. Figure 5 depicts the minima of these effective kernels in the ϕ - θ plane. The dashed line shows the minimum corresponding to the blue twins and the solid line the minimum for the red twins. We note that the minima correspond to different ϕ angles ($45 + \delta$ and $45 - \delta$). The shift δ depends on the parameters of the Landau free energy. Ideally, the red and the blue twins would not run parallel; however, the system accommodates these two conflicting directions by choosing the average angle of 45 degrees. This aspect of competing metastable states is a novel feature associated with the cubic symmetry kernels that leads to a rich landscape of microstructures.

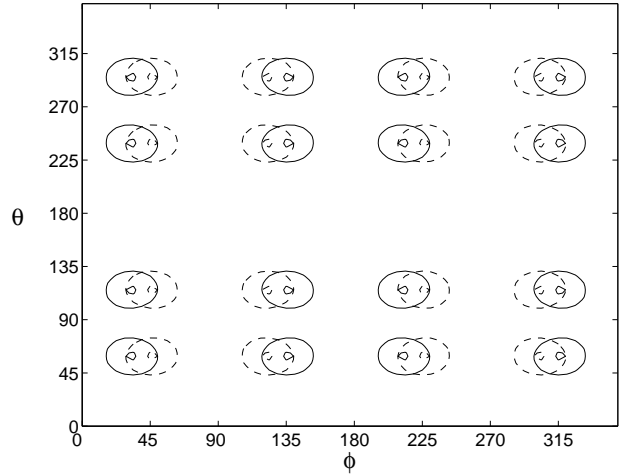


FIG. 5. Minima of effective kernels illustrating inherent strain (orientational) frustration in 3D.

Conclusion. We have derived a complete symmetry based, fully 3D model that describes the cubic to tetragonal structural transitions observed in many martensitic and shape-memory alloys. We obtained analytically the compatibility-induced anisotropic long-range potential in the OP (deviatoric strain tensor components) in the bulk and at interfaces. Unlike the 2D case [11,12], there is a length scale in the system from bulk compatibility alone; the surface compatibility potential also introduces a length scale akin to 2D. Many twin orientations are possible in 3D as a result of elastic frustration and the “landscape” (probably “rugged”) of metastable energy states. Our model can be generalized straightforwardly to improper ferroelastics transitions by including symmetry allowed polarization (magnetization, etc.) nonlinear terms, and couplings to strain. Other symmetries can be handled within our approach. For example, we can study the cubic to trigonal (rhombohedral) transition in lead orthovanadate, and NiTi- and AuCd-based shape-memory alloys using the three shear strains e_4 , e_5 , and e_6 as OP and with e_1 , e_2 , and e_3 expressed in terms of the shear strains via compatibility. Image reconstruction methods of systematic experimental data from HREM and neutron scattering will allow a more quantitative comparison of strain patterns with those obtained from our model.

We wish to thank G. R. Barsch, I. Mitkov, and S. R. Shenoy for insightful discussions. This work was supported by the U.S. Department of Energy (Contract number W-7405-Eng-36). This research used resources of the National Energy Research Scientific Computing Center, which is supported by the Office of Science of the U.S. Department of Energy under Contract No. DE-AC03-76SF00098.

- [1] Z. Nishiyama, *Martensitic Transformations* (Academic, New York, 1978).
- [2] *Shape Memory Effects in Alloys*, edited by J. Perkins (Plenum, New York, 1975).
- [3] J. C. Slonczewski and H. Thomas, *Phys. Rev. B* **1**, 3599 (1970).
- [4] R. D. James, M. Wuttig, *Phil. Mag. A* **77**, 1273 (1998).
- [5] T. Noda, H. Eisaki, and S. Uchida, *Science* **286**, 265 (1999).
- [6] T. Kimura *et al.* **83**, 8733 (1996).
- [7] E. A. H. Love, *A Treatise on the Mathematical Theory of Elasticity* (Dover, New York, 1944), p. 49.
- [8] M. Sugiyama, PhD Thesis, Osaka University, 1985
- [9] D. Schryvers and L. E. Tanner, *Ultramicroscopy* **32**, 241 (1990)
- [10] G. R. Barsch and J. A. Krumhansl, *Phys. Rev. Lett.* **53**, 1069 (1984); *Metallurg. Trans. A* **19**, 761 (1988).
- [11] G. R. Barsch, B. Horovitz, and J. A. Krumhansl, *Phys. Rev. Lett.* **59**, 1251 (1987).
- [12] S. R. Shenoy, T. Lookman, A. Saxena, and A. R. Bishop, *Phys. Rev. B* **60**, R12537 (1999).
- [13] Y. Wang and A. G. Khachaturyan, *Acta Mater.* **45**, 759 (1997).